An 80-W 94.6%-Efficient Multi-Phase Multi-Inductor Hybrid Converter

Ratul Das*, Gab-Su Seo†, Dragan Maksimovic* and Hanh-Phuc Le*
*Department of Electrical, Computer and Energy Engineering, University of Colorado, Boulder, Colorado
†Power Sytems Engineering Center, National Renewable Energy Laboratory, Golden, Colorado
{ratul.das, hanhphuc}@colorado.edu

***Abstract*—This paper presents a new Multi-Phase Multi-Inductor Hybrid (MP-MIH) converter that features high efficiency at large conversion ratios, while operating the switches with duty cycles larger than state-of-the-art hybrid topologies. In this converter, the capacitors are soft-charged and soft-discharged through three inductors operated in three interleaving phases. An experimental six-level three-phase converter prototype achieves 94.6% peak efficiency and 425 W/in^3 power density for conversions from 48V to 1V-2V at loads of up to 40A. This multi-phase multi-inductor hybrid converter architecture can be extended to any number of switched-capacitor network levels to support wide range of input and output voltages and load currents in data centers, telecommunication and other high-performance digital systems.**

***Index Terms*—Hybrid converter, complete soft-charging, switched capacitor network, capacitance optimization, multi phase operation.**

I. Introduction

To bridge a large conversion ratio between input and output voltages, transformer-based topologies have been widely used in point of load (PoL) converters that can provide both high efficiency and high power density for data center and telecom applications as shown in Fig. 1[1]. Transformer-based isolated converters can be constructed by three functional stages. In the first stage, an inverter processes the high input DC voltage to high-frequency AC fed into the primary side of a transformer. The transformer converts this high-voltage AC to a low-voltage AC at the secondary side. The last stage then rectifies the secondary AC to obtain a low-voltage DC. Some of these isolated step-down topologies employ resonance operations to achieve zero voltage switching (ZVS) and/or zero current switching (ZCS) to improve efficiency at the expense of limited, oftentimes fixed, conversion ratios. To maintain fine output regulation at different input voltages, these topologies require supplementary circuits, such as a series-parallel Buck converter [2], pre-regulating ZVS Buck-Boost , or multiphase Buck converter in series with the output [3]. These circuits add significant complexity to design and control, as well as extra losses that limit the overall performance. Among the transformer-based topologies, the Impedance Control Network (ICN) converter can achieve both direct output voltage regulation and resonant operation but its efficiency is still limited to ∼90% for a 48V-to-1.8V conversion [4] .

On the other hand, non-isolated topologies, including the flying-capacitor multi-level (FCML) hybrid converter [5] and

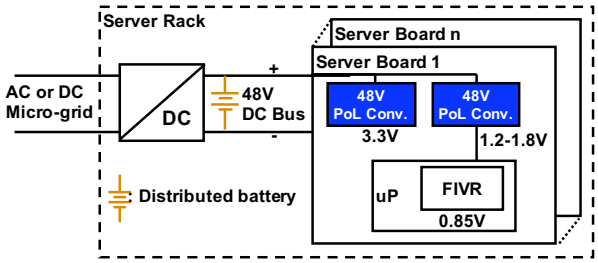

Figure 1. Data center power distribution with PoL converters

Hybrid Dickson switched-capacitor (SC) converter [6], are promising candidates for PoL applications. Both have advantages of complete capacitor soft-charging to obtain high efficiency. However, FCML converter requires extra efforts to balance flying capacitor voltages [5], while Hybrid Dickson SC converter depends upon a split-phase control to achieve high efficiency [6]. Recently, leveraging the intrinsic dual phase operation of the Dickson SC converter, Dual Inductor Hybrid (DIH) converter topologies has been proposed [7], [8]. The DIH converter with odd number of levels excluding the zero level in [8] employs a capacitor sizing strategy to effectively achieve soft-charging and over 91% efficiency for an extreme conversion ratio of 120V-to-1.8V. The even-level DIH converter in [7] utilizes a split-phase operation similar to the Hybrid Dickson SC converter in [6] to minimize hard charging in flying capacitors and achieves ∼95% efficiency for a 48V-to-1.8V conversion.

It is of interest to note that the intrinsic phase duality of a Dickson SC converter can be extended to a larger number of phases to further optimize soft-charging operation [9]. Based on this realization, a Multi-Phase Multi-Inductor Hybrid (MP-MIH) Converter topology is proposed in this paper for PoL applications.Compared with the odd-level DIH converter, MP-MIH converter can achieve complete capacitor soft-charging with a simpler capacitor sizing strategy and does not require any complexity such as split-phase control. In addition, for the same ripple at the output the proposed converter can significantly reduce the inductor size because of its native interleaving operation and small inductor voltage swing, i.e. $\frac{V_{IN}}{N}$ for an N-level MP-MIH converter. In order to explore the capabilities and characteristics of this new converter, we discuss details of the converter operation, capacitor sizing strategy and its advantageous characteristics in Sections II and

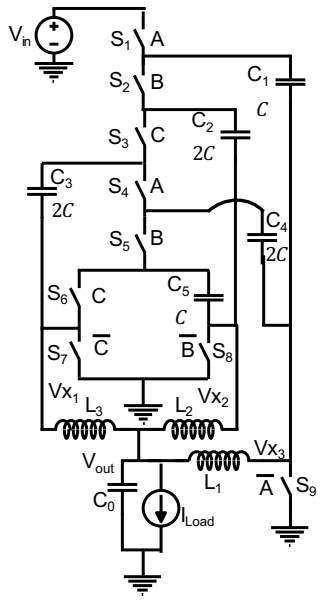

Figure 2. Multi-Phase Multi Inductor Hybrid Converter Topology

III. Section IV presents experimental results of an MP-MIH converter prototype supporting 48V-to-1V/2V conversion at up to 40A loads. Conclusions are presented in Section V.

II. Operation of the Multi-Phase Multi-Inductor Hybrid Converter

A three-phase version of the proposed MP-MIH converter having one inductor for each phase, as shown in Fig. 2, is used to discuss the converter operation principles. The converter consists of five flying capacitors C_{1-5} and eight switches S_{1-8} to form a switched-capacitor network followed by three inductors L_{1-3} and output capacitor C_0. Different from SC converters where flying capacitors are directly connected to the output, the switched capacitor network delivers charges from the input to the output through the three inductors. This configuration enables the hybrid converter to avoid capacitor hard-charging, which is a fundamental loss limitation in SC converters. The converter has three groups of passive components associated with three inductors, L_1 directly connected to C_1 and C_4, L_1 to C_2 and C_5, and L_3 to C_3. As illustrated in Fig. 3 and Fig. 4, the converter has six states with three inductor charging phases in one operating cycle T_S. In States 1, 3, and 5 (Phases A, B, and C), inductors L_1, L_2, and L_3, respectively, get charged. Over a cycle, one inductor charges in one state and discharges (freewheels) to the output in all other states when its associated bottom switch is activated. For example, L_1 gets charged in State 1 (also referred to as Phase A) and discharges in States 2-6. When L_1 gets charged, the capacitors C_1 and C_4 in its group also get charged by the inductor's current in a lossless manner. The charge is then transferred to the next group, L_2 with C_2 and C_5, and finally to L_3 with C_3. In States 2, 4, and 6, all inductors freewheel, while all flying capacitors are open-circuited and inactive. Assuming small ripples on the flying capacitor voltages, the steady state capacitor voltages V_{C1}, V_{C2}, V_{C3}, V_{C4}, and V_{C5} are found to be $\frac{5V_{in}}{6}$, $\frac{4V_{in}}{6}$, $\frac{3V_{in}}{6}$, $\frac{2V_{in}}{6}$, and $\frac{V_{in}}{6}$, respectively, similar to a standard 6-to-1 Dickson switched-capacitor converter [10]. With duty cycle D defined as the ratio between the ON time of one phase and the switching period T_SS, the ideal input to output voltage conversion ratio is $\frac{V_{out}}{V_{in}} = \frac{D}{6}$. The factor 6, enabling a large conversion ratio, comes from the number of levels in the SC network.

As explained above and illustrated in Fig. 3, to maintain the intended operation of the converter Phases A, B, and C need to stay non-overlapped. This limits duty cycle D to $D_{max} = \frac{1}{3}$ and thus, the maximum output voltage to $V_{out,max} = \frac{V_{in}}{18}$. In a general implementation of N-to-1 MP-MIH converter with N SC levels, theoretical output voltage and capacitor voltages are given as:

$$V_{out} = \frac{DV_{in}}{N} \quad \text{and} \quad V_{C_k} = \frac{(N-k)V_{in}}{N} \quad , \quad where, k = 1, 2, ..., N-1 \tag{1}$$

When this MP-MIH converter topology is constructed to have N high-side switches, N-1 capcitors, N levels (ignoring the zero level), M inductors and M charging phases, its duty cycle is limited to $D_{max} = \frac{1}{M}$ and output voltage to $V_{out,max} = \frac{V_{in}}{N \cdot M}$. Note that these non-overlapped interleaving phases need to be equal, i.e. have the same duty cycle D, for intended charge transfer operation and equal inductor current ripple in the inductors. However, they are not required to be evenly distributed over the period. In general, a uniform distribution is preferred since it ensures the smallest current and voltage ripple at the output, as similarly found in multi-phase Buck converters[11].

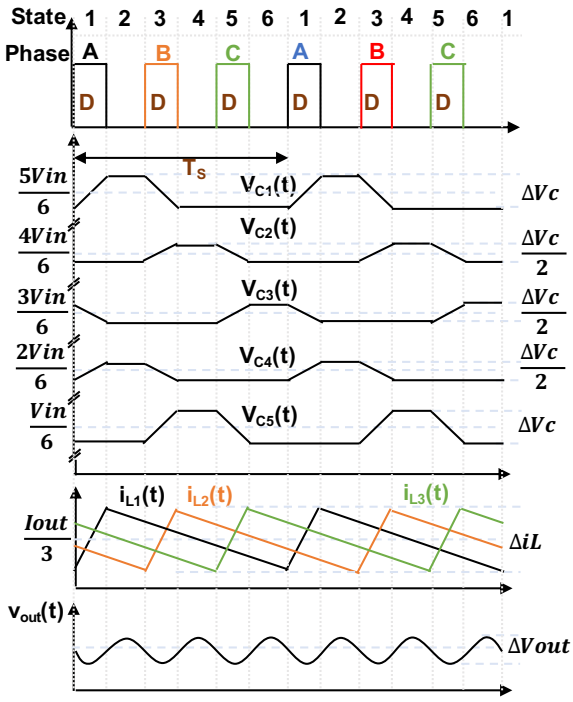

Figure 3. Operational waveforms

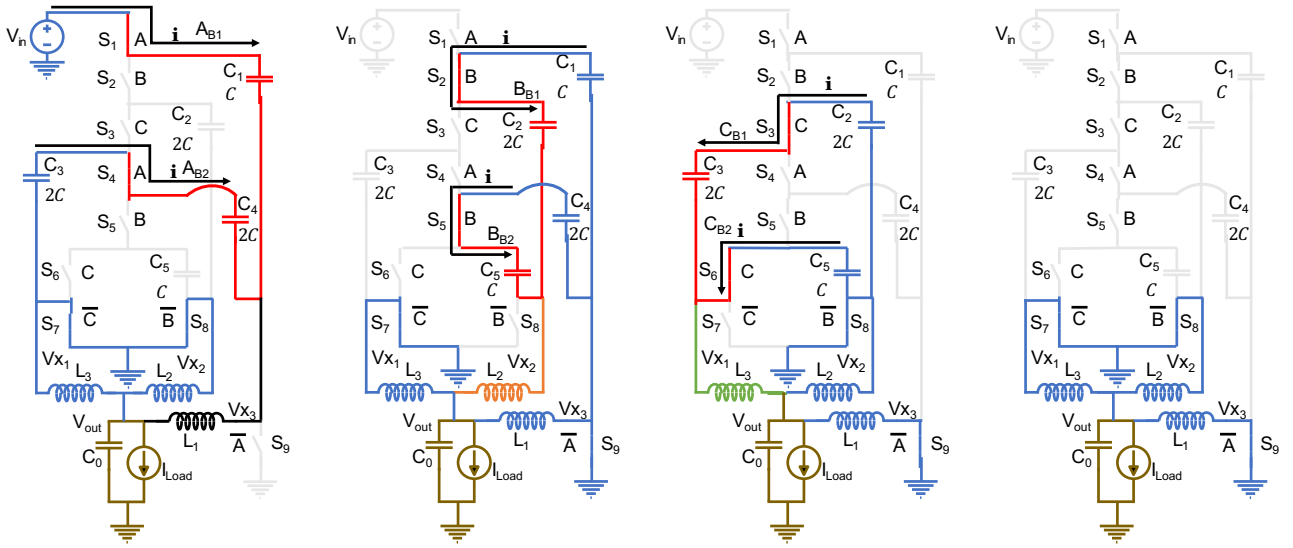

(a) State 1(ϕ A) (b) State 3 (ϕ B) (c) State 5 (ϕ C) (d) State 2,4 and 4(inactive phases)

Figure 4. Operating states of the proposed MP-MIH converter. Capacitors: charged in red, and discharged in blue.

Table I
Equivalent Capacitance Matrix

	Equivalent Capacitances		
Phases	A	B	C
B1 Branches	C_1	$C_1 \parallel C_2$	$C_2 \parallel C_3$
B2 Branches	$C_3 \parallel C_4$	$C_4 \parallel C_5$	C_6

III. Soft-charging operation and strategy for capacitor sizing

In the MP-MIH converter topology, the capacitor charge balance must be met in steady state operation. When the same duty cycle D is applied to Phases A, B and C, the inductors are activated for the same period of time and by the same voltage swing, and thus have the same current level. This results in an identical net charge supplied to each flying capacitor in an active state (State 1, 3, or 5), regardless of phase sequence or effective capacitance values. Note that in the operation of the MP-MIH converter, one inductor is always charged through two capacitor branches in energizing phase A, B, or C. If these two capacitor branches, e.g. C_1 and C_2-C_3 in Phase A have different equivalent capacitances or $C_1 \neq \frac{C_2 \cdot C_3}{C_2+C_3}$, that leads to different inductor current distribution through these branches. In other words, these capacitors will receive different charges distributed by the inductors. To maintain the fundamental steady-state operation of this topology, which assumes that all capacitors process the same net charge, hard-charging may take place at the beginning of active phases to allow for charge redistribution.

Let us first consider a scenario where all the capacitors are sized equally for this converter in the same manner of a Dickson SC converter. In this case, the ripple voltage for each capacitor is $\triangle V_C$, and the switching node voltages generated by individual capacitor branches arelisted in Table II. It can be observed that during States 1 and 5, active capacitor branches do not have equal voltages, which results hard-charging. To remove this undesirable hard-charging, split-phase operation were employed in the Hybrid Dickson topology in [6] and the previous DIH converter topology in [7]. In the split-phase operation, activation of the first and last capacitor branch,

Table II
Switching Node Voltages for Equal Capacitor Sizing

States	Switching Node Voltages	Start	End
1	$Vx_1(A_{B1})$	$\frac{V_{in}}{6}+\frac{\triangle V_C}{2}$	$\frac{V_{in}}{6}-\frac{\triangle V_C}{2}$
	$Vx_1(A_{B2})$	$\frac{V_{in}}{6}+\triangle V_C$	$\frac{V_{in}}{6}-\triangle V_C$
2	$Vx_2(B_{B1})$	$\frac{V_{in}}{6}+\triangle V_C$	$\frac{V_{in}}{6}-\triangle V_C$
	$Vx_2(B_{B2})$	$\frac{V_{in}}{6}+\triangle V_C$	$\frac{V_{in}}{6}-\triangle V_C$
3	$Vx_3(A_{B1})$	$\frac{V_{in}}{6}+\triangle V_C$	$\frac{V_{in}}{6}-\triangle V_C$
	$Vx_3(A_{B2})$	$\frac{V_{in}}{6}+\frac{\triangle V_C}{2}$	$\frac{V_{in}}{6}-\frac{\triangle V_C}{2}$

Table III
Switching Node Voltages for Optimal Ratio Capacitor Sizing

States	Switching Node Voltages	Start	End
1	$Vx_1(A_{B1})$	$\frac{V_{in}}{6}+\frac{\triangle V_C}{2}$	$\frac{V_{in}}{6}-\frac{\triangle V_C}{2}$
	$Vx_1(A_{B2})$	$\frac{V_{in}}{6}+\frac{\triangle V_C}{2}$	$\frac{V_{in}}{6}-\frac{\triangle V_C}{2}$
2	$Vx_2(B_{B1})$	$\frac{V_{in}}{6}+\frac{3\triangle V_C}{4}$	$\frac{V_{in}}{6}-\frac{3\triangle V_C}{4}$
	$Vx_2(B_{B2})$	$\frac{V_{in}}{6}+\frac{3\triangle V_C}{4}$	$\frac{V_{in}}{6}-\frac{3\triangle V_C}{4}$
3	$Vx_3(A_{B1})$	$\frac{V_{in}}{6}+\frac{\triangle V_C}{2}$	$\frac{V_{in}}{6}-\frac{\triangle V_C}{2}$
	$Vx_3(A_{B2})$	$\frac{V_{in}}{6}+\frac{\triangle V_C}{2}$	$\frac{V_{in}}{6}-\frac{\triangle V_C}{2}$

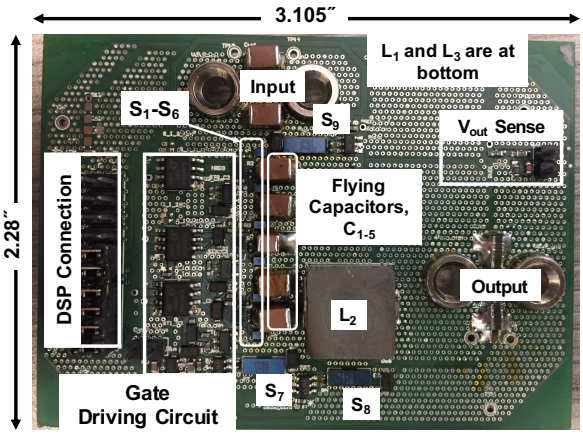

Figure 5. Seven-level Multi-Phase Multi-Inductor Converter prototype

having larger equivalent branch capacitance with only one capacitor of the same size, is made smaller to equalize the net charge delivery to avoid hard charge redistributions. Since the split-phase operation introduces more challenging timing, this may limit possible minimum duty cycles and thus achievable conversion ratios. It is therefore desirable to avoid this hard-charing without using split-phase operation. In the MPMIHC topology, a simple capacitor sizing strategy can be applied to achieve soft charging for the capacitors without using any supplementary operation such as split-phase control. In every active state, there are two branches of capacitors connected with an individual inductor. Particularly, L_1 is connected to two branches of $C_1$and C_3-C_4 in State 1 (Phase A), L_2 to C_1-C_2 and C_4-C_5 in State 2 (Phase B), and $L_3$to C_2-C_4 and C_5 in State 3 (Phase C). Table I lists the equivalent capacitances for these active states. As explained above, to ensure soft charging, active branches in an active state should have the same equivalent capacitance. Therefore, the equivalent capacitances in the two rows of each column in Table I should result in same values. Applying this condition for all capacitor branches in all active states, the required capacitance values can be solved for in terms of a nominal capacitance C as:

$$C_1 = C,\ C_2 = 2C,\ C_3 = 2C,\ C_4 = 2C\ and\ C_5 = C. \quad (2)$$

This capacitor sizing strategy bears similarity to the method used in [8]. However, since in the MP-MIH converter topology in this paper one inductor only handles two capacitor branches instead of three or four branches in **[8]** the approach yields a simpler capacitor sizing calculation and strategy. Particularly,

Table IV
Major Components

Component	Part info.
S_{1-6}	EPC2014c
S_{7-9}	EPC2023
C_1, C_2	2x2.2uF, 4x1.5uF 100V TDK
C_3, C_4, C_5	4x1.5uF, 4x1uF, 2x1uF 50V TDK
L_{1-3}	2.2uH Vishay
Isolators	Si8423
Gate Drivers	LM114BMF, LMG1205YFXR

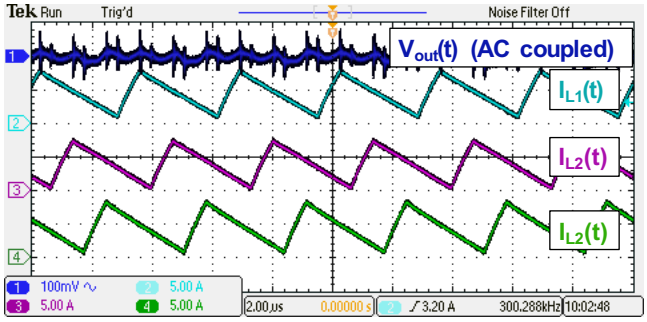

Figure 6. Steady-state waveforms with 13A load current

top capacitor C_1 and bottom-capacitor C_5 in the single capacitor branches should be one half of other capacitors. Using this new capacitor sizes, the switching node voltages are recalculated and tabulated in III, showing uniform capacitor voltages in the branches in each active state effectively eliminating hard-charging.

Although this sizing strategy theoretically ensures no hard-charging, it should be noted that in practice small hard charging may exist because of engineering tolerances and bias voltage-dependent capacitance degradation. In addition, this capacitor sizing strategy does not guarantee valid solutions for all MP-MIH converter versions with any number of phases and levels. For example, there is no valid solution of capacitor values for an eight level four-phase four-inductor converter of this family, but the solution exists for a ten-level five-phase five-inductor version.

IV. EXPERIMENTAL RESULTS

The proposed topology and its operation are verified using the experimental prototype shown in 5 with the components listed in Table IV. Capacitor voltage and inductor current waveforms are shown in Figs. 6 and 7a. Fig. 7b illustrates the flexibility of this converter that the converter maintains its intended operation with different phase sequences. Particularly, the converter is operated with A-B-C sequence in Fig. 7a and with A-C-B sequence in Fig. 7b while maintaining intended characteristics of interleaved inductor phases and soft charging for flying capacitors. The converter has been tested for 48V input voltage and 1V-2V output for up to 40A of load currents, as shown in Fig. 8. It achieves peak efficiency of 94.6% at 2V/8A output and maintains high efficiency (>90%) for a wide range of output loads up to beyond 30A for a 2V output. The converter has a power density of 425 W/in^3 considering key power conversion components.

V. CONCLUSION

The paper describes a Multi-Phase Multi-Inductor Hybrid converter that has significant benefits over state-of-the-art topologies, and shows how SC network can be effectively soft-charged with inductors for high-efficiency conversions. The converter can achieve fine output voltage regulation with a simple pulse-width modulation scheme. In addition, the native interleaving structure and operation in this converter allows it to support high current applications similar to multi-phase

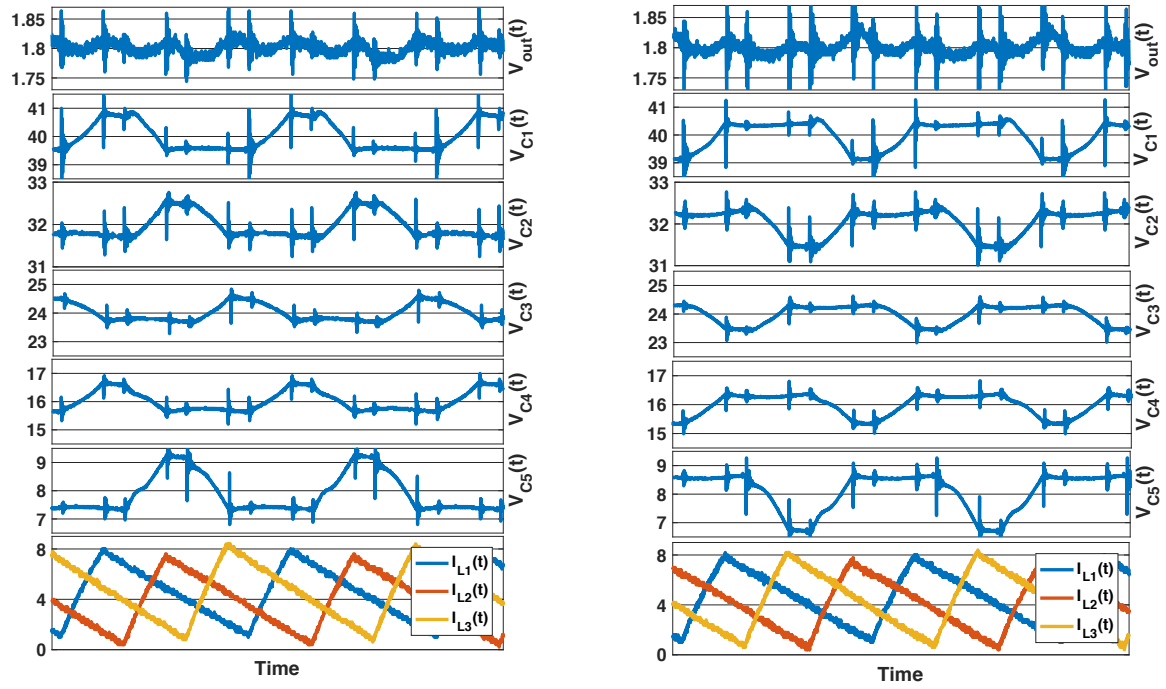

(a) ABC sequence

(b) ACB sequence

Figure 7. Measure Capacitor voltages at 13A loads

Buck converters. A 48V to 1-2V/40A prototype has been demonstrated to achieve 94.6% peak efficiency and 425 W/in^3, promising the MP-MIH converter to be a good candidate for PoL converter applications.

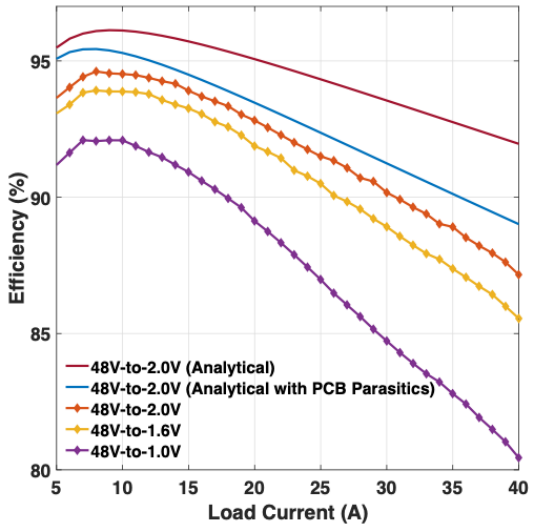

Figure 8. Measured converter efficiency

ACKNOWLEDGMENT

This research work received financial and technical supports from NSF ECCS program award No. 1810470, Oracle, Power America, Lockheed Martin and the University of Colorado Boulder.

REFERENCES

[1] P. T. Krein, "Data Center Challenges and Their Power Electronics," *CPSS Transactions on Power Electronics and Applications*, vol. 2, no. 1, pp. 39–46, Apr. 2017.

[2] M. Ahmed, C. Fei, F. C. Lee, and Q. Li, "High-efficiency high-power-density 48/1v sigma converter voltage regulator module," in *2017 IEEE Applied Power Electronics Conference and Exposition (APEC)*, Tampa, FL, Mar. 2017, pp. 2207–2212.

[3] "Resonant Current Doubler," ST Microelectronics, Tech. Rep.

[4] A. Kumar, S. Pervaiz, and K. K. Afridi, "Single-stage isolated 48v-to-1.8v point-of-load converter utilizing an impedance control network and integrated magnetic structures," in *2017 IEEE 18th Workshop on Control and Modeling for Power Electronics (COMPEL)*, Stanford, CA, Jul. 2017, pp. 1–7.

[5] J. S. Rentmeister and J. T. Stauth, "A 48v:2v flying capacitor multi-level converter using current-limit control for flying capacitor balance," in *2017 IEEE Applied Power Electronics Conference and Exposition (APEC)*, Tamp, FL, Mar. 2017, pp. 367–372.

[6] Y. Lei, Z. Ye, and R. C. N. Pilawa-Podgurski, "A GaN-based 97% efficient hybrid switched-capacitor converter with lossless regulation capability," in *2015 IEEE Energy Conversion Congress and Exposition (ECCE)*, Montreal, QC, Sep. 2015, pp. 4264–4270.

[7] G. S. Seo, R. Das, and H. P. Le, "A 95%-Efficient 48v-to-1v/10a VRM Hybrid Converter Using Interleaved Dual Inductors," in *2018 IEEE Energy Conversion Congress and Exposition (ECCE)*, Portland, Oregon, Sep. 2018.

[8] R. Das, G. S. Seo, and H. P. Le, "A 120v-to-1.8v 91.5%-Efficient 36-W Dual-Inductor Hybrid Converter with Natural Soft-charging Operations for Direct Extreme Conversion Ratios," in *2018 IEEE Energy Conversion Congress and Exposition (ECCE)*, Portland, Oregon, Sep. 2018.

[9] T. Xie, R. Das, G. Seo, D. Maksimovic, and H. P. Le, "Multiphase Control for Robust and Complete Soft-charging Operations of Dual Inductor Hybrid Converter," in *2019 IEEE Applied Power Electronics Conference(APEC))*, Annaheim, Los Angeles, Mar. 2019.

[10] M. D. Seeman and S. R. Sanders, "Analysis and Optimization of Switched-Capacitor DC-DC Converters," *IEEE Transactions on Power Electronics*, vol. 23, no. 2, pp. 841–851, Mar. 2008.

[11] D. Baba, "Benefits of a multiphase buck converter," *Tex. Instrum. Inc.*, 2012.